

# RSC Advances



This is an *Accepted Manuscript*, which has been through the Royal Society of Chemistry peer review process and has been accepted for publication.

*Accepted Manuscripts* are published online shortly after acceptance, before technical editing, formatting and proof reading. Using this free service, authors can make their results available to the community, in citable form, before we publish the edited article. This *Accepted Manuscript* will be replaced by the edited, formatted and paginated article as soon as this is available.

You can find more information about *Accepted Manuscripts* in the [Information for Authors](#).

Please note that technical editing may introduce minor changes to the text and/or graphics, which may alter content. The journal's standard [Terms & Conditions](#) and the [Ethical guidelines](#) still apply. In no event shall the Royal Society of Chemistry be held responsible for any errors or omissions in this *Accepted Manuscript* or any consequences arising from the use of any information it contains.

## **A family of polypropylene glycol-grafted polyethyleneimines reversibly absorb and release carbon dioxide to blow polyurethanes†**

Yuanzhu Long,<sup>‡</sup> Fuhua Sun,<sup>‡</sup> Chao Liu, Xingyi Xie\*

College of Polymer Science and Engineering, Sichuan University, Chengdu, Sichuan 610065, China.

\* Corresponding author: Tel: +86-28-85405129; Fax: +86-28-85405402; E-mail addresses: [xiexingyi@263.net](mailto:xiexingyi@263.net) or [xiexingyi@mail.scu.edu.cn](mailto:xiexingyi@mail.scu.edu.cn) (X. Xie)

<sup>‡</sup> Both authors equally contributed to the paper.

<sup>†</sup> Electronic supplementary information (ESI) available: Details on characterization methods, calculations about grafting rate of PPG-PEIs, and calculations about the theoretical CO<sub>2</sub> content of each CO<sub>2</sub> adduct. See DOI: 10.1039/

Email addresses of other authors:

[125682383@qq.com](mailto:125682383@qq.com) (Y. Long)

[714562196@qq.com](mailto:714562196@qq.com) (F. Sun)

[1172562559@qq.com](mailto:1172562559@qq.com) (C. Liu)

## Abstract

Polyurethane foam community encounters an increasing pressure to replace the ozone depleting and/or global warming blowing agents, like chlorofluorocarbons (CFCs) and hydrochlorofluorocarbons (HCFCs). In this study, a series of polypropylene glycol grafted polyethyleneimines (PPG-PEIs) were synthesised with the grafting rate ranging from 9% to 19%. Their CO<sub>2</sub> adducts (PPG-PEI-CO<sub>2</sub>s) are thermally instable and can release CO<sub>2</sub> to blow polyurethanes whose polymerisation is exothermic. A PPG grafting rate of about 11% (found in sample 1:9-PPG-PEI-CO<sub>2</sub>) is enough to homogenously disperse the blowing agent into polyurethane raw materials. The CO<sub>2</sub> adducts with a PPG grafting rate of about 11–14% are particularly effective to decrease the foam density. The foams blown by 1:9-PPG-PEI-CO<sub>2</sub> possess a thermal conductivity higher than those of traditional polyurethane foams (0.040 vs. 0.020–0.027 W/m·K), hindering their application in thermal insulations. However, these new blowing agents are advantageous in zero emission of volatile organic compounds (VOCs), apart from its climate friendliness. We believe these blowing agents can be used in thermally insulating foams in cars and aircrafts where VOCs are strictly regulated.

**Keywords:** CO<sub>2</sub> adduct, blowing agent, polyethyleneimine, polyurethane foam, climate friendly.

## 1. Introduction

The worldwide demand for polyurethane foams will increase to 13.5 million tonnes in 2016 accounting for 5% of the world consumption of plastics,<sup>1,2</sup> despite the fact that their blowing agents have raised concerns about climate changes.<sup>3-6</sup> Among them, previously used chlorofluorocarbons (CFCs) and hydrochlorofluorocarbons (HCFCs) can severely destroy the stratospheric ozone layer.<sup>3-6</sup> The currently acceptable and popular hydrofluorocarbons (HFCs) are greenhouse gases that contribute to global warming.<sup>6,7</sup>

In response to the climate change concerns, volatile hydrocarbons like cyclopentane<sup>8</sup> and certain unsaturated fluorinated compounds like 1-chloro-3,3,3-trifluoropropene (HCFO-1233zd)<sup>9-11</sup> have been introduced due to their nearly zero ozone depletion potential and very low global warming potential; the latter value is reported as 7 for cyclopentane<sup>4</sup> and 5 for HCFO-1233zd,<sup>11</sup> in contrast to 950 for HFC-245fa (1,1,1,3,3-pentafluoropropane).<sup>7</sup> We recently explored a hydrophobically modified polyethyleneimine which can reversibly absorb and release CO<sub>2</sub> to blow polyurethanes.<sup>12</sup> Poly(propylene glycol) (PPG) chains were grafted onto branched polyethyleneimine (bPEI) backbones, making the resulting PPG-PEI and its CO<sub>2</sub> adduct compatible with PPG polyols which are widely used as raw materials for polyurethane foams. In addition to its climate harmony, this blowing agent releases no volatile organic compounds (VOCs) to atmosphere. This is important in applications like internal car insulation.

In this study, we further optimise the PPG grafting rate of PPG-PEI based blowing agents in order to improve blowing efficiency, while retaining enough raw material compatibility. We believe this optimisation is essential for the real application of this type of

climate friendly blowing agents.

## 2. Materials and methods

### 2.1. Synthesis of polypropylene glycol-grafted polyethyleneimines (PPG-PEIs) and their CO<sub>2</sub> adducts

A series of PPG-PEIs with different grafting rates were synthesised by modifying our previous procedure.<sup>12</sup> Briefly, branched PEI (bPEI,  $M_w = 25,000$  Da by light scattering provided by the supplier) and poly(propylene glycol) monobutyl ether (PPG,  $M_n = 340$  Da) from Sigma–Aldrich served as starting materials. PPG was first transformed into  $\alpha$ -glycidyl ether- $\omega$ -butyl-poly(propylene glycol) (PPG-EPO) by reaction with epichlorohydrin, as described previously.<sup>12</sup> Thereafter, a known amount of PPG-EPO was mixed with 10 g of bPEI in 250 ml of ethanol under stirring. The molar ratio of the epoxy group in PPG-EPO to the amine groups (include primary, secondary and tertiary groups) in bPEI was set as 1:11, 1:9, 1:7 and 1:5, respectively. After reaction at 50 °C for 15 h, the ethanol was rotationally evaporated under reduced pressure. Note that previous synthesis was performed at room temperature for 3 d with the molar ratio set as 1:5 only.<sup>12</sup> The viscous product was dissolved in ethanol/petroleum ether (1/10, v/v) and precipitated with water. The unreacted PPG and PPG-EPO residues were removed by repeatedly washing with petroleum ether. The purified product was named based on the feed molar ratio of epoxy to amine groups, as shown in Fig. 1A, e.g. 1:9-PPG-PEI means the feed molar ratio of epoxy to amine groups is 1:9 in this sample. To prevent them from taking CO<sub>2</sub> and moisture in air, these PPG-PEIs were stored in an N<sub>2</sub>-filled desiccator before any characterisation.

To synthesise the corresponding CO<sub>2</sub> adduct, each PPG-PEI was spread on a piece of release paper and purged with a CO<sub>2</sub> flow under mechanical stirring. The PPG-PEI quickly absorbed the CO<sub>2</sub> and transformed into a white solid in about 1 min. The solid was ground into powder, put into a steel container and saturated with CO<sub>2</sub> at 0.5 MPa for about 1 h. The resulting product was designated by adding “-CO<sub>2</sub>” after the corresponding 1:x-PPG-PEI (x=5, 7, 9, or 11, Fig. 1A), for example 1:11-PPG-PEI-CO<sub>2</sub>, 1:9-PPG-PEI-CO<sub>2</sub>, and so on.

Pure bPEI absorbs CO<sub>2</sub> very slowly (the strong intermolecular H-bonding hindered the permeation of CO<sub>2</sub> and such interaction could be reduced by PPG side chains in PPG-PEIs<sup>12</sup>). Therefore, its CO<sub>2</sub> adduct was synthesised by saturation of 10% bPEI in ethanol with CO<sub>2</sub> at 0.5 MPa for 2 d to form a white precipitate, followed by a complete ethanol evaporation at 40°C for 5 d. This control sample was designated PEI-CO<sub>2</sub>.

## 2.2. Dispersibility of PPG-PEI-CO<sub>2</sub>s in the white component of PU foaming system

Formulation I in Table 1 was used to test the dispersibility of each blowing agent with the rest of the white component. To do so, about 32 g of the white component without any blowing agent (i.e., two folds of Formulation I) was distributed into 6 glass vials with 5 g per vial. Five blowing agents (PEI-CO<sub>2</sub> and 1:x-PPG-PEI-CO<sub>2</sub>, x=5, 7, 9, or 11) were separately added into five of the vials, with 0.156 g per vial. The sixth vial served as a blank control. All liquids in the vials were magnetically stirred at 400 rpm for 2 min. After ageing for 3 d, macroscopic photographs were recorded using a digital camera. The aged samples were shaken to homogenise the mixture. Several drops of each mixture were spread on a glass slide and examined under an Olympus BX 43 light microscope (Olympus, Japan).

**Table 1** The formulation of polyurethane foams

Raw material	Description	Formulation (g)	
		I	II
White component			
Polyether 4110	4-arm poly(propylene glycol), OH number 430 mg KOH/g	8.50	8.50
Silicone L-3102	Foam stabiliser	0.16	0.26
Stannous octoate (T-9)	Catalyst	0.02	0.02
Triethylenediamine (A-33)	Catalyst, 33 wt. % in ethylene glycol	0.20	0.04
Tris(1-chloro-2-propyl) phosphate (TCPP)	Diluent and plasticiser	7.15	7.30
Propylene glycol	Chain extender	0	0.06
Diethanol amine	Cross-linking agent	0	0.20
1:x-PPG-PEI-CO <sub>2</sub>	Blowing agent, x=5, 7, 9, or 11	0.50	3.00
(Total weight)		(16.53)	(19.38)
Black component			
PMDI <sup>a</sup>	NCO content 31wt. %	9.60	15.00

<sup>a</sup> Polymeric 4,4'-diphenylmethane diisocyanate.

### 2.3. Preparation of polyurethane foams

To compare the foaming efficiency of all of the blowing agents (PEI-CO<sub>2</sub> and 1:x-PPG-PEI-CO<sub>2</sub>, x=5, 7, 9, or 11), one set of experiments was conducted using the same formulation (Formulation I, Table 1), but with a change in the blowing agent used. Firstly, all of the raw materials constituting the white component (16.53g, Table 1) were thoroughly mixed in a 250-ml plastic cup by stirring at 1400 rpm for 30 s. Thereafter, 9.6 g of PMDI (black component, Table 1) was added and stirred at the same speed for 15 s. The start of this stirring was set as 0 s. The initially translucent mixture turned white due to the formation of tiny bubbles and rose freely until it became tack free. The whitening time, maximum foam-height time and tack-free time were recorded. Finally, all of the foams were conditioned at room temperature for 4 d before any test.

This set of experiments showed that 1:9-PPG-PEI-CO<sub>2</sub> was the most efficient blowing agent, resulting in the lowest foam density (about 160 kg/m<sup>3</sup>). The foaming art of

1:9-PPG-PEI-CO<sub>2</sub> blown polyurethanes was further modified by ageing the thoroughly mixed white component at room temperature for 3 d. After ageing, PMDI was added to start the foaming process described in the previous paragraph.

To further lower the foam density, we conducted another set of experiments using an increased amount of blowing agents (3.00 g vs. 0.5 g) in the foam formulation (Formulation II, [Table 1](#)) while keeping the main ingredients like polyether 4110 and TCPP almost the same. Compared with Formulation I ([Table 1](#)), more foam stabiliser silicone L-3102 was used because much more bubbles would be generated in the new set of foams. The polymerisation speed was lowered using much less catalyst A-33, to possibly allow a full release of CO<sub>2</sub> prior to foam solidification. Two new ingredients, propylene glycol and diethanol amine as the chain extender and cross-linker, respectively, could enhance the mechanical strength of the rising foams to reduce the breakage of growing bubbles. Moreover, they could assume more PMDI per unit mass than Polyether 4110 because of their low molecular weights. Thus more PMDI was used in Formulation II. This would generate more heat, helping to release CO<sub>2</sub> from the blowing agent. Except for the change in foam formulation, the foaming procedure was the same as described previously for the first set of foams. The whitening time, maximum foam-height time and tack-free time were also recorded.

## 2.4. Characterisations

The details about all the characterisation methods are described in [ESI](#).<sup>†</sup> In brief, the chemical structures of PPG-PEIs and PPG-PEI-CO<sub>2</sub>s were characterised by <sup>1</sup>H nuclear magnetic resonance (NMR) and Fourier transform infrared (FTIR) spectroscopy. The



molecular weights before and after PPG grafting were measured by gel permeation chromatography (GPC). The CO<sub>2</sub> content of each PPG-PEI-CO<sub>2</sub> was determined by thermogravimetry (TG) and the enthalpy change ( $\Delta H$ ) due to the CO<sub>2</sub> release was measured by differential scanning calorimetry (DSC). Both TG and DSC were performed from 30 to 300 °C at 10 °C/min under a nitrogen flow of 100 ml/min. The cellular morphology of PU foams was examined under a scanning electron microscope.

Five replicates ( $n=5$ ) were used to test PU foam density and properties unless otherwise specified. The density was calculated based on the precise weight ( $\pm 0.1$  mg) and dimensions ( $\pm 0.1$  mm) of each sample. The compressive stress–strain curve was recorded on an Instron 5507 Universal Testing Machine at a strain rate of 15% per min (i.e. 3 mm/min) according to ASTM D1621. The thermal conductivity was measured on a Hot Disk TPS 2500-OT thermal analyser. The dimensional stability was measured on cubic samples (about 27 cm<sup>3</sup>) after annealing at 100 °C and –20 °C for 96 h, respectively, according to ISO 2796. The water uptake was determined by the weight change before and after immersion into distilled water at 23 $\pm$ 2 °C for 96 h (ISO 2896), using cubic samples with a volume of about 125 cm<sup>3</sup>. The water vapour permeability was determined by standard method (GB/T 2411) as well.

## 2.5. Statistical analysis

The property data from different groups were compared using a two-tailed Student *t*-test where a significance level of  $p < 0.05$  was accepted.

## 3. Results

### 3.1. Structure and composition of 1:x-PPG-PEI and their CO<sub>2</sub> adducts

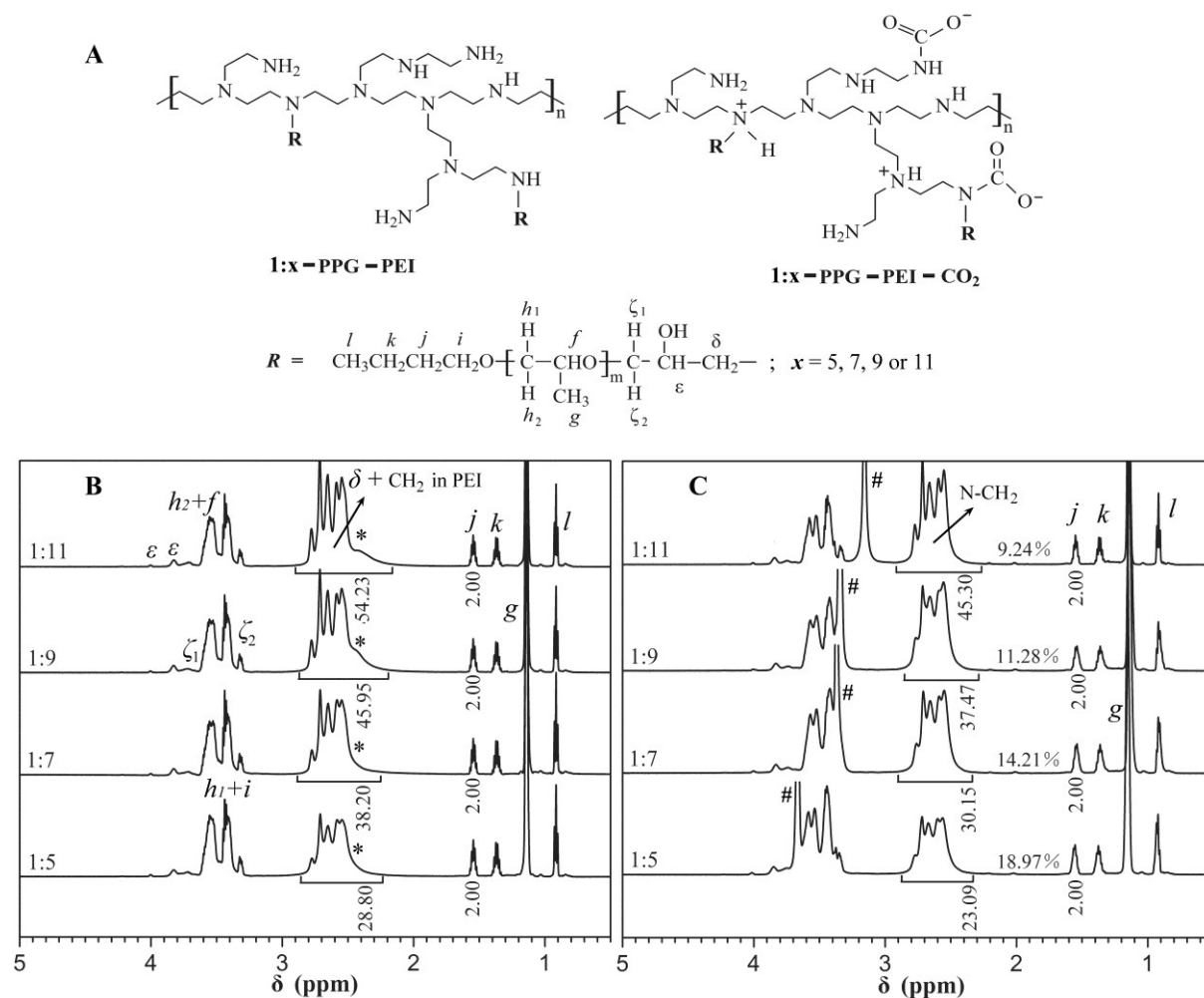


**Fig. 1** <sup>1</sup>H NMR spectra of 1: x-PPG-PEI in CD<sub>3</sub>Cl and in CD<sub>3</sub>Cl+CD<sub>3</sub>OD (5:1, v/v). Relative areas of selected peaks are shown. (A) Chemical structure of the PPG-PEIs and their CO<sub>2</sub> adducts. Here “1: x” refers to the feed molar ratio of PPG molecules to N atoms in PEI. (B) The active proton (N–H and O–H, indicated by \*) signal overlapped with the methylene signals (N–CH<sub>2</sub>, from PEI and H<sub>δ</sub>). (C) The addition of CD<sub>3</sub>OD downfield shifted the active proton signal (indicated by #). Grafting rate is attached on corresponding spectrum.

Shown in Fig. 1B, the <sup>1</sup>H NMR spectra of 1:x-PPG-PEI display characteristic proton signals from both PEI backbones (N–CH<sub>2</sub>, chemical shift at 2.2–2.9 ppm) and PPG side chains (H<sub>f</sub>–H<sub>i</sub>, Fig. 1A). The presence of new signals associated with the linking groups (H<sub>z</sub>, H<sub>ε</sub> and H<sub>δ</sub>,) between the backbones and side chains confirms the success of PPG grafting.<sup>12</sup> The active proton (N–H and O–H, Fig. 1A) signal that initially overlapped with the N–CH<sub>2</sub>

signals was shifted downfield by addition of CD<sub>3</sub>OD in the solvent CD<sub>3</sub>Cl (compare peaks indicated by \* and # in Fig. 1). The relative area of pure N–CH<sub>2</sub> signal (from PEI and H<sub>δ</sub>) was used to calculate the PPG grafting rate (see ESI<sup>†</sup>) which is clearly consistent with corresponding theoretical grafting rate from the feed molar ratio (Table 2). The resultant 1:x-PPG-PEI samples possess high PPG content ranging from 46% to 63.6% (Table 2). The molecular weight obtained from GPC increased as a function of the PPG content in PPG-PEIs, further suggesting that the PPG chains had been grafted onto the PEI backbones.

**Table 2** Important parameters of 1:x-PPG-PEIs and the CO<sub>2</sub> adducts

Parameter	Original PEI	Feed molar ratio in 1:x-PPG-PEI			
		1:11	1:9	1:7	1:5
Grafting rate $\gamma$ (%)					
Theoretical ( $\gamma = 1/x$ )		9.1	11.1	14.3	20.0
Measured <sup>a</sup>		9.2	11.3	14.2	19.0
PPG content (wt. %) <sup>b</sup>		46.0	50.9	56.7	63.6
$M_n$ (10 <sup>4</sup> Da)	2.42	4.30	4.62	5.19	5.87
$M_w$ (10 <sup>4</sup> Da)	3.01	5.57	6.08	6.97	8.20
$M_w/M_n$	1.25	1.30	1.32	1.34	1.40
After conducted with CO <sub>2</sub>					
Theoretical CO <sub>2</sub> content (%) <sup>b</sup>	33.8	21.7	20.1	18.1	15.7
Measured weight loss (%)	33.0	19.4	17.6	14.3	12.5
PPG content (wt. %) <sup>b</sup>		37.1	41.9	48.6	55.7
Measured $\Delta H$ (J/g)	367	185	177	154	124
Normalised $\Delta H$ (J/g) <sup>b</sup>		294	305	300	280

<sup>a</sup> From 1H NMR spectra, see ESI<sup>†</sup>.

<sup>b</sup> The calculation of these parameters is shown in ESI<sup>†</sup>. The theoretical CO<sub>2</sub> contents are calculated based on the fact that two amino groups or two repeating units capture one CO<sub>2</sub> molecule. The normalised  $\Delta H$  is calculated by excluding the mass of PPG side chains in each 1:x-PPG-PEI-CO<sub>2</sub>, and just based on the mass of the PEI-CO<sub>2</sub> backbones.

The FTIR spectra of 1:x-PPG-PEI also confirm their chemical structure (Fig. 2A). For instance, typical N–H bending from PEI and C–O–C stretching from PPG are identified at 1652 cm<sup>-1</sup> and 1114 cm<sup>-1</sup>, respectively. The intensity of PPG methyl bending at 1375 cm<sup>-1</sup> (\* indicated, Fig. 2A) increased from 1:11- to 1:5-PPG-PEI, consistent with the increase of PPG

content across these samples (Table 2).

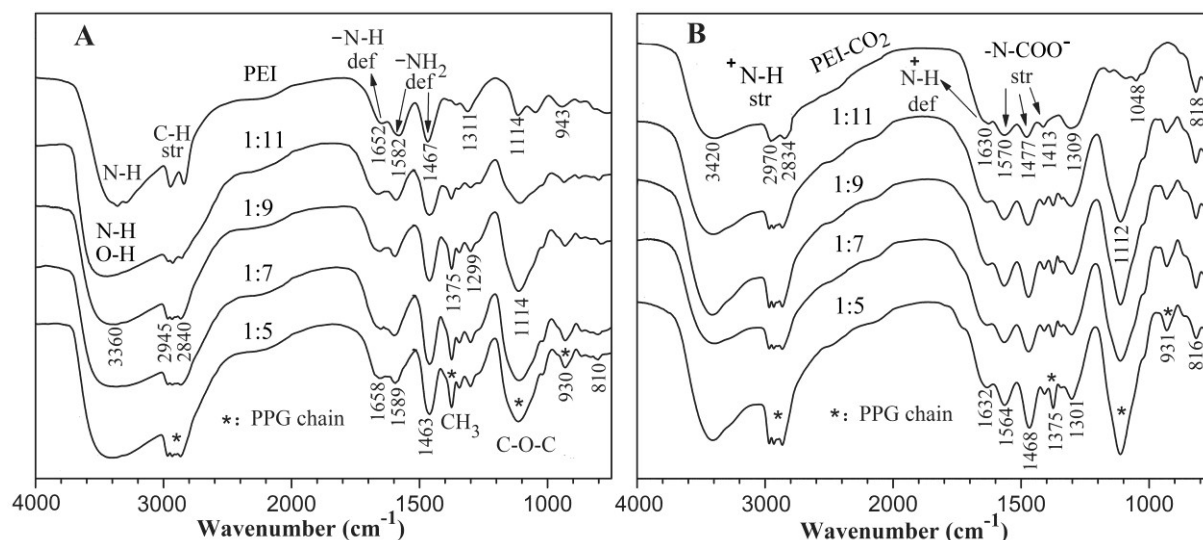


**Fig. 2** The FTIR spectra of PEI and 1: x-PPG-PEI (A) and their CO<sub>2</sub> adducts (B). The absorptions related to PPG chains (\*) became more prominent with the increase of PPG content (i.e. the decrease of x).

The CO<sub>2</sub> adducted samples displayed the same change trend in PPG methyl band (Fig. 2B). The CO<sub>2</sub> adduction generated alkylammonium cations and carbamate anions (>NCOO<sup>-</sup> and -NHCOO<sup>-</sup>) (Fig. 1A) in the PEI backbones. This can be confirmed by a series of strong IR absorption bands at about 1630, 1570, 1477 and 1413 cm<sup>-1</sup> (Fig. 2B), resulting from N-H bending in the alkylammoniums,<sup>13</sup> C=O stretching in the carbamates,<sup>13</sup> the asymmetrical and symmetrical skeletal stretching of the carbamate anions,<sup>13-15</sup> respectively. The changes in IR spectra before and after CO<sub>2</sub> adduction agree with the results reported previously.<sup>12</sup>

Fig. 3 shows TG and DSC curves of the CO<sub>2</sub> adducts. Negligible weight loss and zero enthalpy change ( $\Delta H$ ) were observed in the control sample 1:5-PPG-PEI. The weight loss and endothermic process observed in the CO<sub>2</sub> adducts can be associated with their CO<sub>2</sub> release upon heating, as both showed the same temperature range for each sample (compare Fig. 3A and B). The measured weight loss in PEI-CO<sub>2</sub> is very close to its theoretical CO<sub>2</sub> content (33.0% vs. 33.8%, Table 2), showing complete CO<sub>2</sub> absorption in this sample. Other samples

possessed slightly lower weight loss than corresponding theoretical CO<sub>2</sub> content (Table 2). Both measured weight loss and measured  $\Delta H$  decreased from 1:11- to 1:5-PPG-PEI-CO<sub>2</sub>. However, the normalised  $\Delta H$ 's which excluded the weight of PPG side chains were similar across these samples (Table 2).

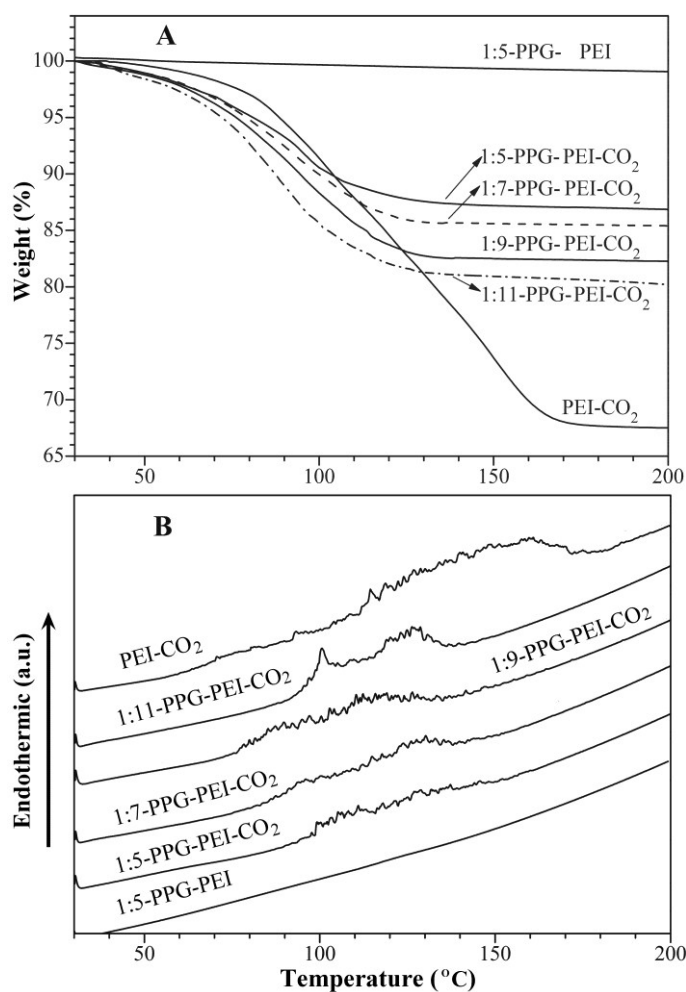
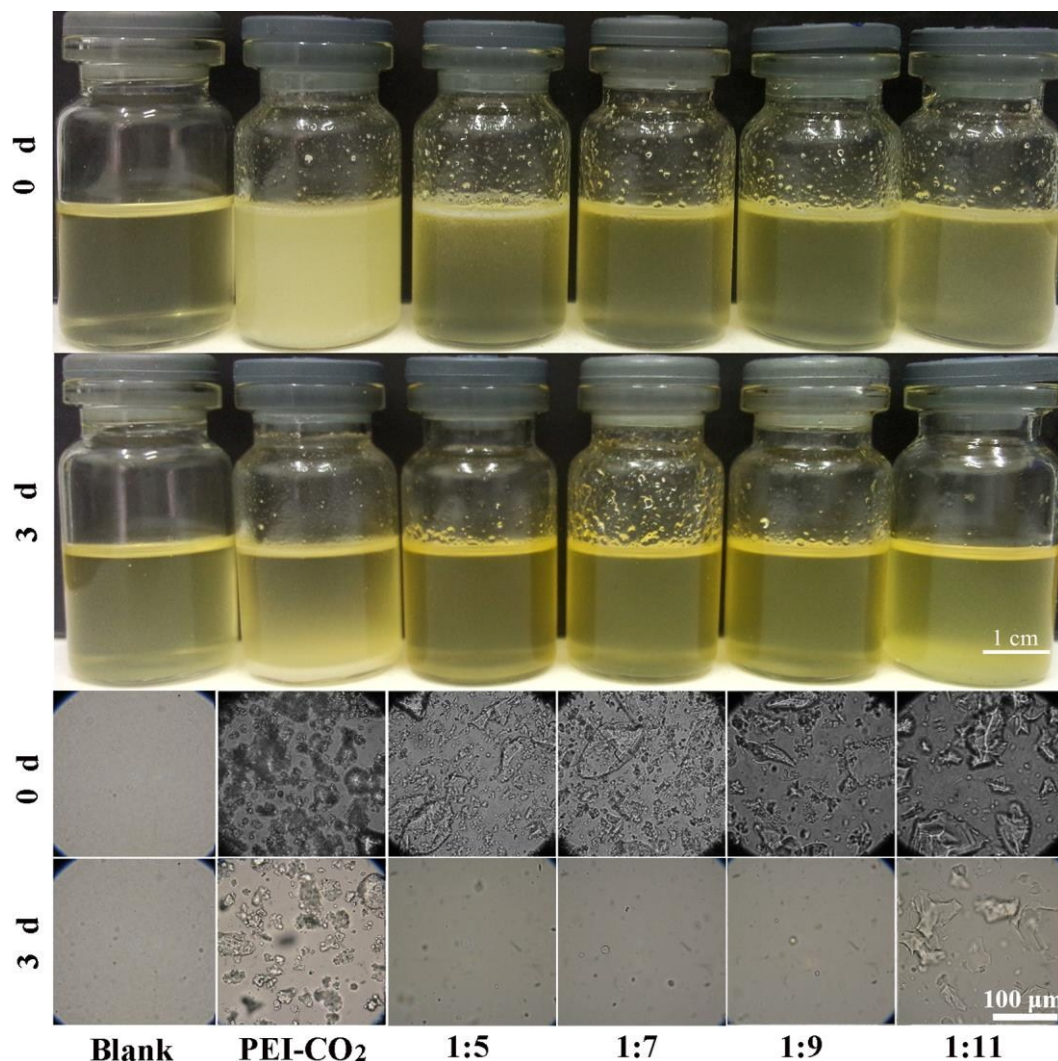


**Fig. 3** TG (A) and DSC (B) curves of the CO<sub>2</sub> adducts and the control (1:5-PPG-PEI). The weight loss of each adduct indicates the corresponding CO<sub>2</sub> content. PPG grafting lowers the CO<sub>2</sub> releasing temperatures and narrows their range. Negligible weight loss (0.6% before 150 °C) and zero enthalpy were observed in 1:5-PPG-PEI.

Among all CO<sub>2</sub> adducts, PEI-CO<sub>2</sub> displayed the widest temperature range of CO<sub>2</sub> release spanning from 60 to 180 °C (Fig. 3B). Overall, PPG grafting decreased the upper limit of CO<sub>2</sub> release range by about 30 °C. Sample 1:9-PPG-PEI-CO<sub>2</sub> demonstrated the lowest initial

release temperature (at  $\sim 70$  °C) among the PPG-grafted samples.

### 3.2. Dispersibility of the CO<sub>2</sub> adducts in polyurethane foam raw materials



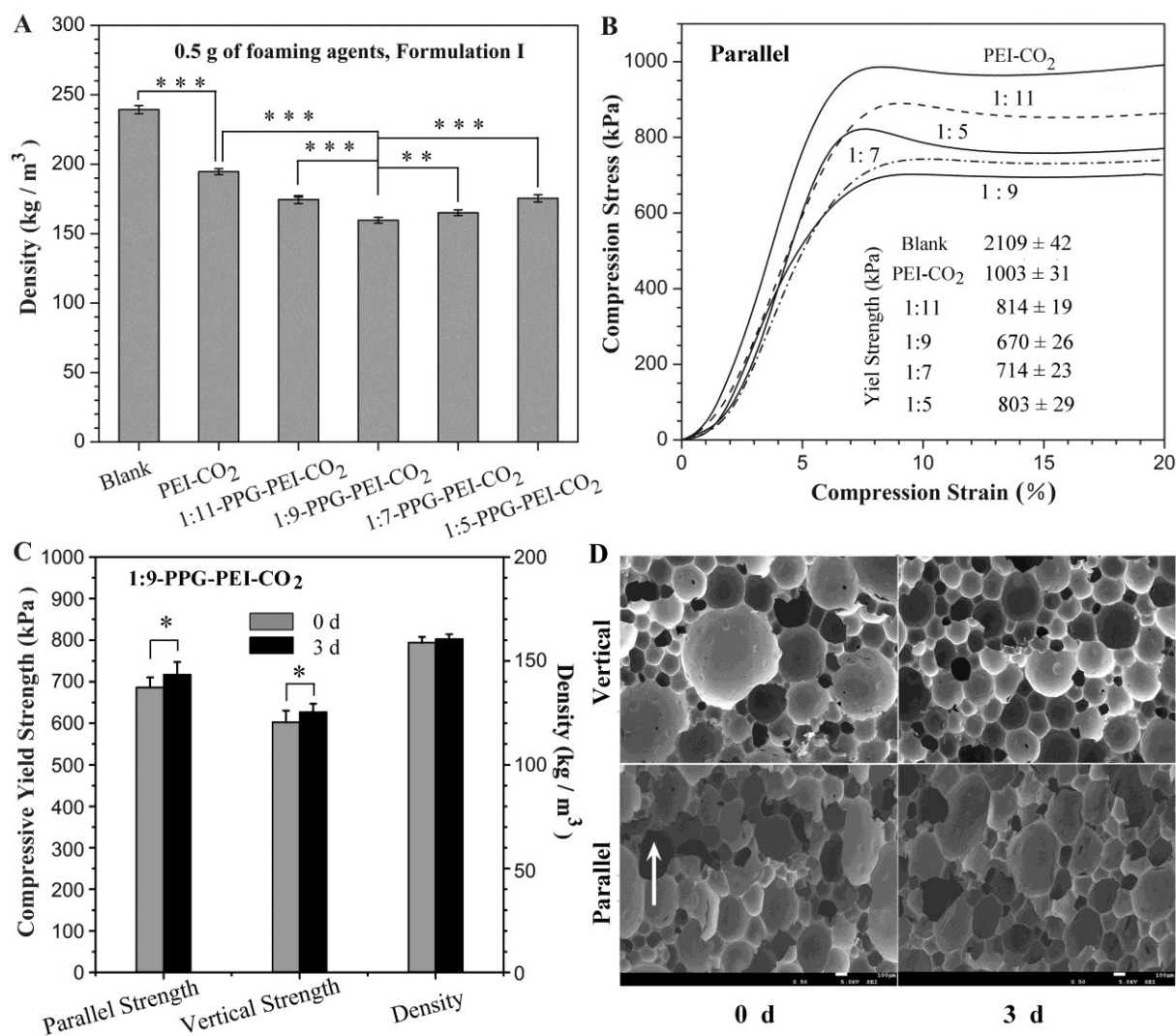
**Fig. 4** Evolution of macroscopic and microscopic photographs of the white components (Formulation I, Table 1) with and without the CO<sub>2</sub> adducts, after stirring at 400 rpm for 2 min.

Fig. 4 shows macroscopic and microscopic photographs of the white components (Formulation I, Table 1) with and without the blowing agents. The control sample without any blowing agent (Blank) was clear, showing no phase separation and no suspending particles during the entire experiment. PEI-CO<sub>2</sub> displayed the worst dispersibility, as confirmed by the initially turbid and later precipitated appearance. Sample 1:11-PPG-PEI-CO<sub>2</sub> demonstrated a

subsiding layer for the same period, with a more blurred interface compared with that in PEI-CO<sub>2</sub> sample. Microscopically, some large and irregular particles still remained in both PEI-CO<sub>2</sub> and 1:9-PPG-PEI-CO<sub>2</sub> samples. Samples with 1:5-, 1:7- and 1:9-PPG-PEI-CO<sub>2</sub> retained a translucent appearance for at least 3 d. Likewise, their microscopic images demonstrate a significant decrease in number and size of visible particles. Taking into consideration both macroscopic and microscopic observations, the dispersibility of all samples can be ranked as 1:5-  $\approx$  1:9-  $\approx$  1:7- > 1:11-PPG-PEI-CO<sub>2</sub> > PEI-CO<sub>2</sub>.

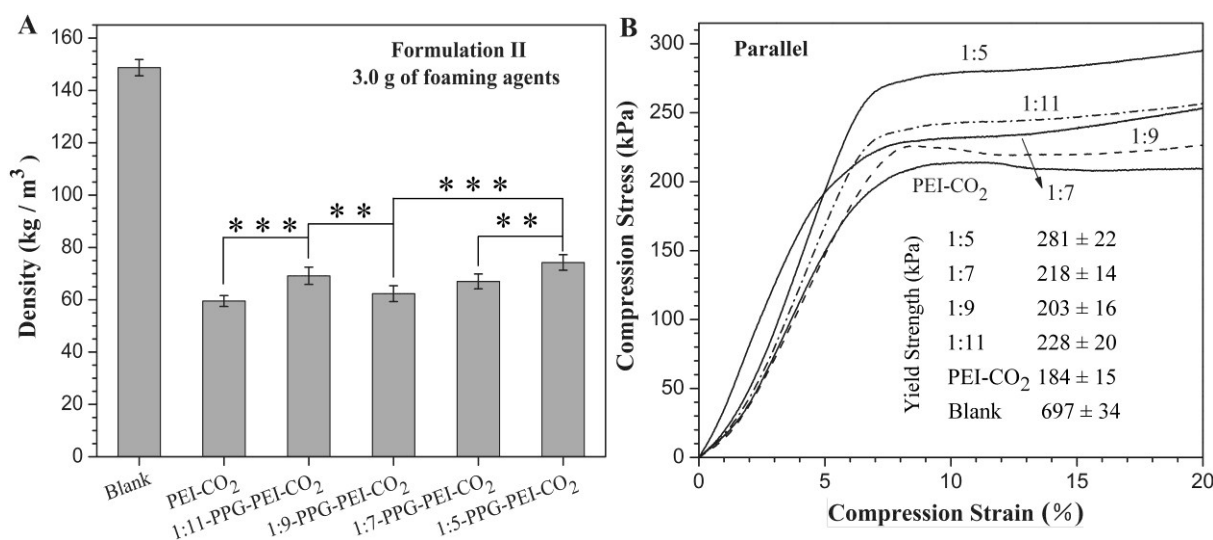
### 3.3. Polyurethane foaming with different blowing agent

Fig. 5 compares density and mechanical strength of polyurethane foams based on Formulation I (Table 1). All foams using the CO<sub>2</sub> adducts as blowing agents displayed a lower density than the blank foam blown by water impurity in the raw materials, with the lowest density ( $159.7 \pm 2.2$  kg/m<sup>3</sup>) found in 1:9-PPG-PEI-CO<sub>2</sub> blown foam (Fig. 5A). The compressive strength positively correlated with the foam density, with the lowest strength occurring in 1:9-PPG-PEI-CO<sub>2</sub> blown sample as well (Fig. 5B). Represented by this sample, white component ageing improved the compressive strength (Fig. 5C), while keeping the density statistically the same. In addition, both mechanical and morphological anisotropy were observed, independent of the white component ageing. The compressive strength at the foam rise direction was higher than that at the vertical direction (Fig. 5C). The vertical cross-sections displayed round pores, in contrast with an elliptical morphology parallel to the foam rise direction (Fig. 5D).



**Fig. 5** Property and morphology of polyurethane foams prepared with Formulation I (Table 1). \*\*\*:  $P < 0.001$ ; \*\*:  $P < 0.01$ ; \*:  $P < 0.05$ . (A) The foams blown by 1:9-PPG-PEI-CO<sub>2</sub> possessed the lowest density among all the foams (measured with five samples i.e.  $n = 5$ ). (B) The compressive yield strength at the foam rise direction (Parallel) varied mainly depending on the sample density. (C, D) The anisotropic mechanical strength and anisotropic morphology observed in 1:9-PPG-PEI-CO<sub>2</sub> blown foams, with the white component aged for 0 or 3 d. The foam rise direction (Parallel) is indicated by a white arrowed line. The white component ageing enhanced the mechanical strength ( $n = 10$ , C), lowered and homogenised the pore size of the foams (D), but kept the densities statistically the same ( $P > 0.05$ ,  $n = 10$ , C). Scale bars in D: 100  $\mu\text{m}$ .





**Fig. 6** Density and compressive strength of polyurethane foams prepared with Formulation II (Table 1). The compression tests (measured with five samples) were conducted at the foam rise direction. \*\*\*:  $P < 0.001$ ; \*\*:  $P < 0.01$ .

**Table 3** Parameters of the foaming process based on Formulation I and II

Blowing agent	Whitening time (s)		Maximum foam-height time (s)		Tack-free time (s)	
	I	II	I	II	I	II
Blank <sup>a</sup>	26	60	90	259	105	495
PEI-CO <sub>2</sub>	18	44	78	195	94	325
1:11-PPG-PEI-CO <sub>2</sub>	19	48	80	212	95	354
1:9-PPG-PEI-CO <sub>2</sub>	22	51	82	230	97	422
1:7-PPG-PEI-CO <sub>2</sub>	23	53	85	264	98	485
1:5-PPG-PEI-CO <sub>2</sub>	25	55	85	279	100	504

<sup>a</sup> Without blowing agent used.

Another set of foams was prepared based on Formulation II (Table 1). Since more blowing agent was used in this set of experiments (3.0 g vs. 0.5 g), the catalyst A-33 content was significantly lowered to decrease the polymerisation speed and to allow a possibly full release of CO<sub>2</sub>. This polymerisation slowdown was confirmed by the much longer whitening time, foam rising time and track-free time than those in the first set of experiments (Table 3). The blank sample displayed a much lower density than that in previous experiments (148.7 kg/m<sup>3</sup> vs. 239.3 kg/m<sup>3</sup>, Table 4), showing more water present in the raw materials for this set

of samples. Addition of the CO<sub>2</sub> adducts significantly decreased the foam density and compressive strength as expected (Fig. 6 and Table 4). The density of CO<sub>2</sub> adduct-blown samples varied narrowly between 59 and 74 kg/cm<sup>3</sup>. The 1:9-PPG-PEI-CO<sub>2</sub> blown foam possessed a similar density with PEI-CO<sub>2</sub> and 1:7-PPG-PEI-CO<sub>2</sub> blown samples ( $P > 0.05$ , Fig. 6A). However, its density was statistically lower than those of 1:11- and 1:5-PPG-PEI-CO<sub>2</sub> blown foams.

**Table 4** The entrapped CO<sub>2</sub> amount compared with that of theoretically released CO<sub>2</sub> during PU foaming

Blowing agent <sup>a</sup>	Density (kg/m <sup>3</sup> )	Foam volume (cm <sup>3</sup> )	Entrapped CO <sub>2</sub> <sup>b</sup> (ml)	Theoretically released CO <sub>2</sub> <sup>c</sup> (ml)	Foaming efficiency <sup>d</sup> (%)
0.5 g, Formulation I					
Blank	239.3 ± 2.9	109.19		0	
PEI-CO <sub>2</sub>	194.6 ± 2.2	134.28	25.09	117.90	21.3
1:11-PPG-PEI-CO <sub>2</sub>	174.5 ± 1.9	149.74	40.55	69.31	58.5
1:9-PPG-PEI-CO <sub>2</sub>	159.6 ± 2.2	163.72	54.53	62.88	86.7
1:7-PPG-PEI-CO <sub>2</sub>	165.0 ± 2.1	158.36	49.17	51.09	96.2
1:5-PPG-PEI-CO <sub>2</sub>	175.5 ± 2.6	148.89	39.70	44.66	88.9
3.0 g, Formulation II					
Blank	148.7 ± 3.1	231.20		0	
PEI-CO <sub>2</sub>	59.5 ± 2.1	577.82	346.62	688.94	50.3
1:11-PPG-PEI-CO <sub>2</sub>	69.2 ± 3.3	496.82	265.62	405.02	65.6
1:9-PPG-PEI-CO <sub>2</sub>	62.4 ± 3.0	550.96	319.76	367.43	87.0
1:7-PPG-PEI-CO <sub>2</sub>	66.0 ± 2.8	520.91	289.71	298.54	97.0
1:5-PPG-PEI-CO <sub>2</sub>	73.3 ± 3.0	469.03	237.83	260.96	91.1

<sup>a</sup> No blowing agent was used in blank samples.

<sup>b</sup> Calculated by subtracting blank foam volume from each foam volume.

<sup>c</sup> Calculated based on the moles of CO<sub>2</sub> (CO<sub>2</sub> content from TG curve) in each blowing agent, the highest temperature of foaming process (about 110 °C and 100 °C for Formulation I and II, respectively) and the standard air pressure ( $P = 101325$  Pa), using the ideal gas law as  $PV = nRT$ .

<sup>d</sup> Obtained from entrapped CO<sub>2</sub> volume divided by theoretically released CO<sub>2</sub> volume.

It is reasonable that the net increase in foam volume relative to the blank sample stands for the CO<sub>2</sub> volume trapped within the corresponding foam. Similarly, the percentage of

trapped CO<sub>2</sub> relative to theoretically released CO<sub>2</sub> from each CO<sub>2</sub> adduct indicates the foaming efficiency. Shown in Table 4, PEI-CO<sub>2</sub> and 1:11-PPG-PEI-CO<sub>2</sub> demonstrated relatively low foaming efficiencies (21–66%) while 1:9-, 1:7- and 1:5-PPG-PEI-CO<sub>2</sub> possessed foaming efficiencies of about 87% or over.

Table 5 compares the properties of 1:9-PPG-PEI-CO<sub>2</sub> blown foams with those required for applications in thermal insulation. The foam properties should be further optimised for these applications; in particular, the thermal conductivity should be lowered.

**Table 5** The properties of 1:9-PPG-PEI-CO<sub>2</sub> blown foams from Formulation II, in comparison with the data from Chinese standards

Property	Measured	Required properties for thermal insulation <sup>a</sup>		
		Building walls	Refrigerators	Underground steel pipes
Density (kg/m <sup>3</sup> )	62.4 ± 3.0	≥30	28~35	40~60
Compressive strength (kPa)	203 ± 16	≥100	≥100	≥100
Thermal conductivity (W/m·K)	0.040 ± 0.002	≤0.027	≤0.022	≤0.03
Dimensional changes (%) <sup>b</sup>				
-20 °C for 96 h	Length	-0.96 ± 0.05		
	Width	-1.17 ± 0.02	≤1	
	Height	1.31 ± 0.13		
100 °C for 96 h	Length	-1.14 ± 0.05		
	Width	-3.71 ± 0.20	≤5	≤1.5
	Height	2.11 ± 0.13		≤3
Water uptake (v/v %)	2.3 ± 0.1		≤5	≤3
Water vapour permeability (ng/m·s·Pa)	7.22 ± 1.24	≤6.5		

<sup>a</sup> Obtained from Chinese standards GB/T 10800, GB/T 2081 and SY/T 0415, respectively; <sup>b</sup> The height is parallel to foam rise direction. The minus data indicate shrinkage, and the controlled dimensional changes are given as absolute values.

## 4. Discussion

### 4.1. CO<sub>2</sub> release temperatures and raw material compatibility of the CO<sub>2</sub> adducts

We previously confirmed that 1:5-PPG-PEI-CO<sub>2</sub> can release CO<sub>2</sub> to blow polyurethanes.<sup>12</sup> To find better blowing agents, we changed the PPG grafting rate of the CO<sub>2</sub> adduct whose chemical structure was confirmed by <sup>1</sup>H NMR and FTIR spectra (Figs. 1 and 2).

The consistency between measured and theoretical values in both PPG grafting rate and CO<sub>2</sub> content, and the increase in molecular weight after PPG grafting (Table 2) clearly indicates the success in material synthesis.

The weight loss (Fig. 3) of CO<sub>2</sub> adducts was an endothermic process caused by the decomposition of alkylammonium carbamates in the main chain that released CO<sub>2</sub>. The PPG grafting resulted in a decrease in primary amine-derived carbamate anions (–NHCOO<sup>–</sup>) in corresponding CO<sub>2</sub> adduct because PPG grafting can preferentially consume primary amines in original PEI. The –NHCOO<sup>–</sup> groups decompose at higher temperatures than >NCOO<sup>–</sup> groups due to extra H-bonds among the former. Therefore, the decomposition temperature range of PEI-CO<sub>2</sub> (with more –NHCOO<sup>–</sup> anions) extended up to 180 °C, about 30 °C higher than the upper limit of other CO<sub>2</sub> adducts (Fig. 3). Accordingly, the normalised  $\Delta H$ s in 1:x-PPG-PEI-CO<sub>2</sub> were lower than the measured  $\Delta H$  in PEI-CO<sub>2</sub> (Table 2).

The PPG side chains in 1:x-PPG-PEI-CO<sub>2</sub> tended to expose to the liquid portion of the white component that contains a similar PPG polyol (polyether 4110, Table 1), which drove the dispersion of the CO<sub>2</sub> adducts (Fig. 4). Both macroscopic and microscopic observation showed that samples 1:9-, 1:7- and 1:5-PPG-PEI-CO<sub>2</sub> are compatible with the liquid white component while 1:11-PPG-PEI-CO<sub>2</sub> and PEI-CO<sub>2</sub> are not dispersible. The grafting rate of about 11% in 1:9-PPG-PEI-CO<sub>2</sub> (Table 2) is enough to generate a homogeneous foaming mixture for PU foams.

#### 4.2. Effects of PPG content on the foaming process

As shown in Table 3, the increase in PPG content decreased the foaming speed in both

sets of experiments; the whitening time, maximum foam-height time and tack-free time were all roughly delayed with the increase of PPG content from 0% in sample PEI-CO<sub>2</sub> to 63.6% in sample 1:5-PPG-PEI-CO<sub>2</sub> (Table 2). This might be explained by insight into the foaming process, where the blowing agent released increasing amounts of CO<sub>2</sub> and gradually restored its original polyamine structure. The restored free amines quickly reacted with isocyanate groups in the growing polyurethane chains and/or catalysed the chain growth, accelerating the exothermic polymerisation, thus speeding up the CO<sub>2</sub> release. Due to the steric hindrance caused by PPG side chains, such an acceleration effect decreased with the increased PPG content. So did the foaming speed.

The slowdown in foaming speed allows a more complete release of CO<sub>2</sub> before the foam solidification. This partially accounts for the rough increase in foaming efficiency from 1:11- to 1:5-PPG-PEI-CO<sub>2</sub> (Table 4). The highest upper limit of CO<sub>2</sub> release temperatures in PEI-CO<sub>2</sub> (Fig. 3) might have prevented it from completely releasing CO<sub>2</sub> during the foaming process. The poorest dispersibility of this sample (Fig. 4) resulted in the most inhomogeneous release of CO<sub>2</sub>; those relatively large bubbles might have broken up before the foam was set. All of these factors led to the lowest foaming efficiency in PEI-CO<sub>2</sub> despite its highest CO<sub>2</sub> content. For 1:11-PPG-PEI-CO<sub>2</sub>, its poor dispersibility was also responsible for its low foaming efficiency. Samples 1:9-, 1:7- and 1:5-PPG-PEI-CO<sub>2</sub> could more completely release CO<sub>2</sub> during the foaming process because of their similarly low CO<sub>2</sub> release temperatures (Fig. 3). Their relatively higher dispersibility (Fig. 4) and thus more homogenous release of CO<sub>2</sub> would inhibit the formation of very large bubbles with high potential to break, facilitating the improved foaming efficiency, which was in the range from 86% to 97%.

The large decrease in foaming speed from Formulation I to Formulation II (Table 3) caused an obvious increase in foaming efficiency in both PEI-CO<sub>2</sub> and 1:11-PPG-PEI-CO<sub>2</sub> (Table 4). On the other hand, samples 1:9-, 1:7- and 1:5-PPG-PEI-CO<sub>2</sub> displayed a stable and high foaming efficiency, regardless of the change in foaming formulation. In this case, the foaming efficiencies of PEI-CO<sub>2</sub> and 1:11-PPG-PEI-CO<sub>2</sub> were still much lower than those of 1:9-, 1:7- and 1:5-PPG-PEI-CO<sub>2</sub> (Table 4). Again, the insufficient and/or inhomogeneous release of CO<sub>2</sub> still occurred in both PEI-CO<sub>2</sub> and 1:11-PPG-PEI-CO<sub>2</sub> foaming systems.

Overall, a homogeneous CO<sub>2</sub> release resulting from the high dispersibility of the CO<sub>2</sub> adduct and a match between the polymerisation speed and the CO<sub>2</sub> release rate are key factors for a high foaming efficiency. This was the case for the 1:7-PPG-PEI-CO<sub>2</sub> foaming system, which displayed a foaming efficiency as high as 96–97% (Table 4). The slightly lower foaming efficiencies (87–91%) found in 1:9- and 1:5- PPG-PEI-CO<sub>2</sub> can be improved by finely adjusting the foaming formulation, e.g. using more foam stabiliser to avoid bubble breakage before foam solidification.

The foam density depends on the CO<sub>2</sub> content (Table 2) and the foaming efficiency (Table 4) of each blowing agent. The polyurethanes blown by 1:9-PPG-PEI-CO<sub>2</sub> were among the least dense foams (Figs. 5 and 6). Only PEI-CO<sub>2</sub> and 1:7-PPG-PEI-CO<sub>2</sub> blown polyurethanes based on Formulation II had similar density ( $P > 0.05$ , Fig. 6A and Table 4). Currently, both 1:7- and 1:9-PPG-PEI-CO<sub>2</sub> are acceptable in terms of good dispersibility and high foaming efficiency. Taking into consideration the higher CO<sub>2</sub> content and its potential to further improve the foaming efficiency, 1:9-PPG-PEI-CO<sub>2</sub> can be the most promising candidate for real applications.

The compressive strength is generally related to the density (Figs. 5B and 6B). However, the white component ageing for 3 days promoted the dispersion of 1:9-PPG-PEI-CO<sub>2</sub>, thereby lowering and homogenising the pore size of the resultant foams (Fig. 5D). This morphological change did not affect the foam density but improved the compressive strength (indicated by \*, Fig. 5C). The anisotropic morphology with the major axes of the elliptical pores pointing to the foam rise direction (Fig. 5D) is due to the horizontal confinement of the foam expansion by the container wall. As a result, the compressive strengths at the foam rise direction were larger than across it, both before and after the white component ageing (Fig. 5C). These observations clearly confirm that not only the foam density but also the porous morphology affects the mechanical strength.

#### 4.3. Possible applications and future investigations

In fact, the foams prepared in this study belong to rigid polyurethane foams (whose yield strain < 10%, Figs. 5B and 6B) with closed individual pores (Fig. 5D). Their potential applications are as structural materials or as thermal insulation materials. As shown in Table 5, most of the current properties of 1:9-PPG-PEI-CO<sub>2</sub> blown foams approximate to those required for insulating underground steel pipes. For the other two applications (building wall and refrigerator insulation), the foam density should be further lowered; this might be achieved by using more blowing agent in the formulation. Accordingly, the resultant compressive strength would be lowered to some extent, and it is not difficult to satisfy the required value of  $\geq 100$  kPa as the current strength is about 200 kPa (Table 5).

The dimensional change of the current foam is suitable for building wall insulation, but

not acceptable for insulations of refrigerators and underground steel pipes (Table 5). The roughly higher shrinkage perpendicular to foam rise direction than expansion parallel to it suggests a reduced pressure in the individual foam pores resulting from a fast outward diffusion of CO<sub>2</sub> and a slow inward diffusion of air.<sup>16</sup> This diffusion mismatch has been reported by Tseng et al.<sup>17</sup> in a 25-mm thick polyurethane foam blown by CO<sub>2</sub> and CFC 11 (1:1, by v/v) where CO<sub>2</sub> completely diffused out in about 3 days, while the volume of air infiltrated for about 1 month (almost no diffusion of CFC 11 was observed in the same period). The anisotropic dimension change is related to the anisotropic mechanical strength (Fig. 5C) showing that the foams are more easily compressed horizontally (i.e. perpendicular to foam rise direction). The dimensional change can be reduced by ageing the foams for a longer time (e.g. for one month) and/or by improving the mechanical strength via optimisation in foaming art (e.g. ageing the white component to homogenise the pore size, Fig. 5C and D).

A major obstacle for application in thermal insulations is the relatively high current thermal conductivity (Table 5). According to previously proposed models,<sup>17-19</sup> the thermal conductivity ( $K$ ) of a foam material is calculated by:

$$K = K_g + 2K_s\rho_f/3\rho_s + 16\sigma T^3/3(42.038\rho_f + 121.55) \quad (1)$$

where  $\rho$ ,  $T$  and  $\sigma$  stands for density, average absolute temperature and the Stefan-Boltzman constant ( $5.67 \times 10^{-8} \text{ W/m}^2 \cdot \text{K}^4$ ), respectively, and the subscript g, s and f indicates gas phase, solid phase and the whole foam, respectively. For polyurethanes, the typical  $K_s$  and  $\rho_s$  is 0.262 W/m·K and 1200 kg/m<sup>3</sup>, respectively.<sup>19</sup> The  $K_g$  of CO<sub>2</sub> and air at 298.15 K is 0.0166 and 0.0257 W/m·K, respectively.<sup>20</sup> Substituting the density of the 1:9-PPG-PEI-CO<sub>2</sub> blown



polyurethane ( $62.4 \text{ kg/m}^3$ , Table 5) and other parameters into equation (1), one obtains the thermal conductivity of fresh foams (the trapped gas was  $\text{CO}_2$ ) as  $0.0286 \text{ W/m}\cdot\text{K}$ . However, with the replacement of  $\text{CO}_2$  by air due to diffusion, the thermal conductivity finally increases to the value of an air-filled foam which is calculated as  $0.0377 \text{ W/m}\cdot\text{K}$ . The measured value ( $0.040 \pm 0.002 \text{ W/m}\cdot\text{K}$ ) is consistent with this calculated value, showing the trapped  $\text{CO}_2$  had been completely replaced by air when measuring the thermal conductivity.

Equation (1) shows that the thermal conductivity is density-dependent; the minimum value reaches  $0.0358 \text{ W/m}\cdot\text{K}$  at about  $33 \text{ kg/m}^3$  for the air-equilibrated foams, decreasing by only  $0.002 \text{ W/m}\cdot\text{K}$  compared with the calculated value at  $62 \text{ kg/m}^3$ . Lowering density is not an effective way to decrease the thermal conductivity. The minimum value is even higher than the upper limit of the required thermal conductivities in standards (Table 5). Therefore, the current foam is not suitable for the applications listed in Table 5, just taking into account the thermal insulation property.

Traditional blowing agents (CFCs, HCFCs and HFCs) on the one hand possess very low thermal conductivity (e.g. HCFC 141b:  $0.01 \text{ W/m}\cdot\text{K}$ ; CFC 11:  $0.0082 \text{ W/m}\cdot\text{K}$ )<sup>20</sup> and on the other hand diffuse very slowly through polyurethane foams (the diffusion coefficients of  $\text{CO}_2$ ,  $\text{N}_2$  and  $\text{O}_2$  are two to three orders of magnitude higher than those of HCFCs and CFCs).<sup>21</sup> Therefore, the out-diffusion of traditional blowing agents can last for years,<sup>22, 23</sup> helping to preserve the low thermal conductivity of the foams. For instance, a 1 cm-thick polyurethane foam blown by HCFC 141b still retains a thermal conductivity below  $0.026 \text{ W/m}\cdot\text{K}$  after a 2-year ageing at  $32.2 \text{ }^\circ\text{C}$ .<sup>22</sup>

The thermal conductivity ( $0.040 \text{ W/m}\cdot\text{K}$ ) of 1:9-PPG-PEI- $\text{CO}_2$  blown polyurethane

foams is comparable to those of expanded polystyrene (0.029–0.041 W/m·K), but higher than those of traditional polyurethane foams (0.020–0.027 W/m·K).<sup>24</sup> The benefits due to zero emission of climate changing substances in the new blowing agents and the benefits due to the higher thermal resistance in traditional blowing agents should be comprehensively compared in terms of climatic impact, for example using life cycle analysis,<sup>7, 25</sup> which considers all impacts during the manufacturing processes and the overall life cycle of the corresponding foam product.

The long-term release of blowing agents from traditional polyurethane foams can limit their application as thermal insulation materials in a closed or semi-closed environment (e.g. in cars, trains and aircrafts) where the local concentration of VOCs is strictly regulated.<sup>26, 27</sup> In this case, the new polyurethane foam in this study is a good alternative.

## 5. Conclusion

A series of CO<sub>2</sub> adducts from polypropylene glycol-grafted polyethyleneimines were synthesised as climate-friendly blowing agents for polyurethanes. A grafting rate of 11% or higher facilitated a homogenous disperse of the CO<sub>2</sub> adduct in the raw materials of polyurethane foams. Foams blown by 1:9- and 1:7-PPG-PEI-CO<sub>2</sub> (with a PPG grafting rate of 11.3% and 14.2%, respectively) displayed the lowest foam density when the same amount of each blowing agent was used. The current thermal conductivity of the resultant foams is higher than those of traditional polyurethane foams (0.040 vs. 0.020–0.027 W/m·K). Besides their climate neutrality, these new blowing agents do not release any VOCs, making them good candidates as thermal insulation materials in closed and semi-closed environments like

in cars and aircrafts.

## Acknowledgments

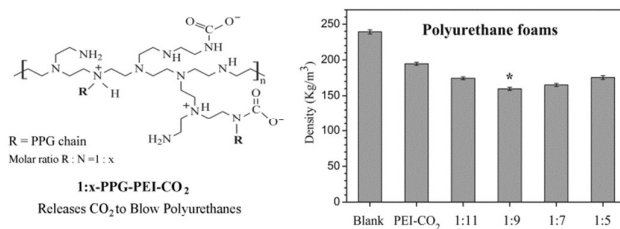
This work was financially supported by the National Natural Science Foundation of China (Grant No. 51173111). Ms. Hui Wang from the Analytical Centre, Sichuan University, China, helped to observe the SEM images, which is highly appreciated.

## References

- 1 A. Cornille, S. Dworakowska, D. Bogdal, B. Boutevin and S. Caillol, *Eur. Polym. J.*, 2015, 66, 129–138.
- 2 H. Singh and A. K. Jain, *J. Appl. Polym. Sci.*, 2008, 111, 1115–1143.
- 3 V. Naik, A. K. Jain, K. O. Patten and D. J. Wuebbles, *J. Geophys. Res.*, 2000, 105, 6903–6914.
- 4 L. D. D. Harvey, *Build. Environ.*, 2007, 42, 2860–2879.
- 5 K.-H. Kim, Z.-H. Shon, H. T. Nguyen and E.-C. Jeon, *Atmos. Environ.*, 2011, 45, 1369–1382.
- 6 G. J. Velders, S. O. Andersen, J. S. Daniel, D. W. Fahey and M. McFarland, *PNAS*, 2007, 104, 4814–4819.
- 7 A. McCulloch, *J. Cell. Plast.*, 2009, 46, 57–72.
- 8 W. Bazzo, A. Cappella and S. Talbot, *J. Cell. Plast.*, 1996, 32, 46–61.
- 9 F. Molés, Navarro-Esbrí J., B. Peris, A. Mota-Babiloni, Á. Barragán-Cervera and K. Kontomaris, *Appl. Therm. Eng.*, 2014, 71, 204–212.
- 10 Y. K. Ling and D. J. Williams, *US Pat. 9,000,061 B2*, 2015.
- 11 R. J. Hulse, R. S. Basu, R. R. Singh and R. H. P. Thomas, *J. Chem. Eng. Data* 2012, 57, 3581–3586.
- 12 Y. Long, L. Zheng, Y. Gu, H. Lin and X. Xie, *Polymer*, 2014, 55, 6494–6503.
- 13 N. Hiyoshi, K. Yogo and T. Yashima, *Micropor. Mesopor. Mat.*, 2005, 84, 357–365.
- 14 X. Wang, V. Schwartz, J. C. Clark, X. Ma, S. H. Overbury, X. Xu and C. Song, *J. Phys. Chem. C*, 2009, 113, 7260–7268.
- 15 G. Qi, Y. Wang, L. Estevez, X. Duan, N. Anako, A.-H. A. Park, W. Li, C. W. Jones and E. P. Giannelis,

- Energy Environ. Sci.*, 2011, 4, 444–452.
- 16 C. Cecchini, R. Zannetti and A. Stefani, *J. Cell. Plast.*, 1999, 35, 514–530.
  - 17 C. Tseng, M. Yamaguchi and T. Ohmorit, *Cryogenics*, 1997, 37, 305–312.
  - 18 A. G. Leacht, *J. Phys. D Appl. Phys.*, 1993, 26, 733–739.
  - 19 W. H. Tao, H. C. Hsu, C. C. Chang, C. L. Hsu and Y. S. Lin, *J. Cell. Plast.*, 2001, 37, 310–332.
  - 20 H. Macchi-Tejeda, H. Opatovà and J. Guilpart, *Int. J. Refrig.* 2007, 30, 338–344.
  - 21 M. C. Page and L. R. Glicksman, *J. Cell. Plast.*, 1992, 28, 268–283.
  - 22 K. E. Wilkes, W. A. Gabbard, F. J. Weaver and J. R. Booth, *J. Cell. Plast.*, 2001, 37, 400–428.
  - 23 K. E. Wilkes, D. W. Yarbrough, W. A. Gabbard and G. E. Nelson, *J. Cell. Plast.*, 2002, 38: 317–339.
  - 24 A. M. Papadopoulos, *Energ. Buildings*, 2005, 37, 77–86.
  - 25 R. W. Johnson, *Int. J. Refrig.*, 2004, 27, 794–799.
  - 26 K. Brodzik, J. Faber, D. Łomankiewicz and A. Gołda-Kopek, *J. Environ. Sci.*, 2014, 26, 1052–1061.
  - 27 C. Wang, X. D. Yang, J. Guan, K. Gao and Z. Li, *Build. Environ.*, 2014, 78, 89–94.

## Graphical Abstract



The chemical structure of CO<sub>2</sub> adducts from polypropylene glycol grafted polyethyleneimines has been optimised to blow polyurethanes.